Anal. Chem. **1997,** *69,* 728−733

High-Throughput Fast-Scan Anodic Stripping Voltammetry in a Microflow System

Feimeng Zhou,* Joseph T. Aronson, and Max W. Ruegnitz

Department of Chemistry, University of Wisconsin—Eau Claire, Eau Claire, Wisconsin 54702

A flow-onto thin-layer electrochemical cell, incorporating Pt-based Hg microelectrodes, is used for fast-scan anodic stripping voltammetry (FS-ASV) at microbore flow rates. The slow flow rates are uniformly altered and controlled utilizing a gas displacement pump. Flow injection is carried out with a low-dead-volume six-port valve. In such a microflow system, the high precision that is observable in quiescent solutions is maintained. The detection limits (e.g., 0.17 nM for Cd^{2+} with a 2-min preconcentration, or 0.19 pg of Cd^{2+} at 4.9 μL/min) are remarkably lower than those previously reported in other flow systems utilizing Hg microelectrodes. Compared to ASV in quiescent solutions and in other flow systems, this setup has an excellent sample throughput and low sample consumption. For example, at moderately fast scan rates (e.g., 15 V/s), one analysis of a sample containing Pb^{2+} or Cd^{2+} at submicromolar levels takes about 10 s, with only 0.82 μL of sample consumed. Experimental conditions that govern the sensitivity, sample consumption, and throughput are discussed (i.e., scan rate, flow rate, Hg film thickness, and preconcentration time). Finally, potential use of this device for automatic analyses is demonstrated.

In recent years, the application of microelectrodes to stripping analysis (SA) has attracted a great deal of attention.[1−18] Previous studies have demonstrated that the utilization of microelectrodes for SA resulted in the elimination of sample deoxygenation and stirring in the preconcentration step,[4] miniaturization and simplification of the instrumentation,[4,5,11−13,16−17] and undistorted stripping voltammograms from highly resistive media.[8] Compared to SA conducted at conventional-sized Hg drop and thin Hg film electrodes in quiet solutions,[19−21] some important analytical aspects of SA, such as precision,[3] signal-to-noise ratio,[1,3] sample consumption,[4,5,17] and throughput,[16] have also been significantly improved. Initially, major emphasis was placed on the use of carbon fiber and/or carbon fiber-based Hg microelectrodes[1,2,4−10] because of the relatively high hydrogen overpotential and the reproducibility in forming thin Hg films at the carbon surface. Baranski conducted rapid potentiometric stripping analysis[4] and fast-scan anodic stripping voltammetry (FS-ASV)[5] at carbon fiber disk microelectrodes or carbon fiber-based Hg microelectrodes. In those studies, an analysis conducted in a quiescent solution required only 5 μL of sample.[4] Detection limit for Cd^{2+} was determined to be about 5 nM at 10 V/s using only a 10-s preconcentration.[5] The feasibility of Pt-based Hg microelectrodes for routine ultratrace SA was first demonstrated by Wehmeyer and Wightman.[3] Excellent precision ranging from 1.0 to 3.0% relative standard deviation (%RSD) was obtained. It was also shown that spherical Hg droplets can be easily made at Pt substrates.[3] Since Hg microelectrodes formed at Pt substrates are found to be more hydrodymamically stable[15−17] than those based on carbon substrates, Pt-based Hg microelectrodes have been favored for the purpose of SA in flowing solution streams,[16,17] despite the fact that Pt tends to cause more intermetallic compounds to form in the Hg microelectrodes.

Pt thin-ring-based Hg microelectrodes were first used by Tay et al. in a flow injection system with solution flowing at a few milliliters per minute.[16] The good precision observed in quiescent solutions was found to be maintained in their flow injection ASV experiments. However, the sample consumption was high due to the fast solution flow rates, and the analyte concentrations determined were at micromolar levels. Matysik and Werner designed a novel flow injection system in which microbore flow rates (microliters per minute or less) could be used.[17] Coupled with differential pulse voltammetry, sample consumption was dramatically reduced (1.4 μL for each injection). The major disadvantages of their setup are its low sample throughput (at least 7 min were needed for one analysis) and the difficulty for automation (a micropositioner was needed to place the Pt microelectrode close to the solution inlet). Furthermore, the concentration levels determined (about 60 nM for Cd^{2+}), though lower than those found with the flow injection experiment at fast flow rates, are almost 2 orders of magnitude higher than those that can be obtained in quiescent solutions. Since higher mass

(1) Cushman, M. R.; Bennett, N. G.; Anderson, C. W. *Anal. Chem. Acta* **1981**, *130*, 323.
(2) Schulze, G.; Frenzel, W. *Anal. Chim. Acta* **1984**, *159*, 95.
(3) Wehmeyer, K. R.; Wightman, R. M. *Anal. Chem.* **1985**, *57*, 1989−1993.
(4) Baranski, A. S.; Quon, H. *Anal. Chem.* **1986**, *58*, 407.
(5) Baranski, A. S. *Anal. Chem.* **1987**, *59*, 662−670.
(6) Gołas, J.; Osteryoung, J. *Anal. Chim. Acta* **1986**, *181*, 211−218.
(7) Gołas, J.; Osteryoung, J. *Anal. Chim. Acta* **1986**, *186*, 1−9.
(8) Wang, J.; Zadeii, J. M. *J. Electroanal. Chem.* **1988**, *246*, 297−305.
(9) Wang, J.; Peng, T. *Anal. Chim. Acta* **1987**, *197*, 367.
(10) Wang, J.; Peng, T.; Zadeii, J. *Anal. Chem.* **1987**, *59*, 2119−2122.
(11) Harman, A. R.; Baranski, A. S. *Anal. Chim. Acta* **1990**, *239*, 35−44.
(12) Wojciechowski, M.; Balcerzak, J. *Anal. Chim. Acta* **1990**, *237*, 127−133.
(13) Wojciechowski, M.; Balcerzak, J. *Anal. Chim. Acta* **1991**, *249*, 433−445.
(14) Amez del Pozo, J.; García, C. A.; Blanco, P. T. *Anal. Chim. Acta* **1993**, *273*, 101−109.
(15) Matysik, F.-M.; Gläser, P.; Werner, G. *Analyst* **1994**, *349*, 646−649.
(16) Tay, E. B.-T.; Khoo, S.-B.; Loh, S.-W. *Analyst* **1989**, *114*, 1039−1042.
(17) Matysik, F.-M.; Werner, G. *Analyst* **1993**, *118*, 1523−1526.
(18) Wikmark, G.; Lejon, J.; Nyholm, L. *Water Chemistry of Nuclear Reactor Systems*; British Nuclear Energy Society: London, 1992; Vol. 6, No. 2, pp 219−222.
(19) Wang, J. *Stripping Analysis-Principles, Instrumentation and Applications*; VCH: Deerfield Beach, FL, 1985.
(20) Vydra, F.; Štulík, K.; Juláková, E. *Electrochemical Stripping Analysis*; Wiley: Chichester, Sussex, U.K., 1976.
(21) Wiederin, D. R.; Smith, F. G.; Howk, R. S. *Anal. Chem.* **1991**, *63*, 219−225.

S0003-2700(96)00763-9 CCC: $14.00

transport in flowing solution streams should enhance the preconcentration efficiency, it is clear that the methodology of flow injection ASV needs to be improved for more rapid and sensitive detections.

It is, therefore, desirable to develop a simple flow injection SA system that has high throughput, small sample consumption, and low detection limits. We report here the combination of a microflow system consisting of a low-flow-rate solution delivery module and a low-dead-volume six-port injection valve with a miniaturized flow-onto thin-layer electrochemical cell. Fast linear scan voltammetry, for the first time, is used as a rapid and sensitive detection method for flow SA. The aim of this work was to develop a practical system that has the capability of performing ultratrace analysis at nanomolar levels with microliter sample consumption. In this study, we also examined the parameters affecting the analytical performance of the flow injection FS-ASV and demonstrated the improvement in several analytical aspects of the flow SA based on Hg microelectrodes.

EXPERIMENTAL SECTION

Reagents and Chemicals. High-purity elemental standard solutions were purchased from Aldrich (Milwaukee, WI). Nitric acid used for preparing the carrier solution was doubly distilled from Vycor (GFS Chemicals, Columbus, OH). Hexaammineruthenium(III) chloride ($Ru(NH_3)_6Cl_3$) was obtained from Strem Chemicals (Newburyport, MA). Water used to prepare the solutions was purified by a Barnstead system (Boston, MA).

Instruments. The Microneb 2000 solvent delivery/flow injection system (CETAC Technologies Inc., Omaha, NE), designed for flow injection analysis using inductively coupled plasma mass spectrometry detection,[22] can be easily modified for flow injection FS-ASV. Figure 1a is a schematic diagram showing the combination of Microneb 2000 with the thin-layer flow-onto electrochemical cell that is controlled by a computer-driven potentiostat. The Microneb 2000 consists of a gas displacement pump (GDP), a low-dead-volume six-port valve, and a peristaltic pump. Solution flow rates and sample loading/injection are controlled by a microcomputer module. The GDP has the capability of delivering solutions at flow rates ranging from a few microliters per minute to a few milliliters per minute without pulsations. To achieve microbore flow rates with the GDP, Teflon-encapsulated-PEEK tubings (127 μm i.d., CETAC Technologies Inc.) were used to introduce the necessary backpressure. In Figure 1a, the Teflon-encapsulated-PEEK tubing (127 μm i.d.) that was used to connect the six-port valve and the GDP reservoir had a length of 116 cm, and the piece that was connected to the cell outlet was 22 cm long. To minimize the delivery time for the injected sample to the cell, a much shorter tubing (7 cm long or 0.7 μL) was used to connect the cell to the valve. Uniform, pulsation-free solution flow is critical for obtaining quantitative and reproducible ASV data at microelectrodes. The peristaltic pump, prone to serious pulsations, is used only to fill the sample loop and the carrier solution reservoir of the GDP.

The potentiostat employed was either an Ensman EI 400 bipotentiostat (Ensman Instruments, Bloomington, IN) or a CHI 832 electrochemical analyzer (CH Instruments, Cordova, TN). The EI 400 bipotentiostat was controlled by a 486 PC using software developed for the control of a scanning electrochemical microscope (CE-6000, generously provided by Prof. David Wipf).

(22) Wightman, R. M.; Wipf, D. O. In *Electroanalytical Chemistry*; Bard, A. J., Ed.; Marcel Dekker: New York, 1989; Vol. 15, pp 267−353.

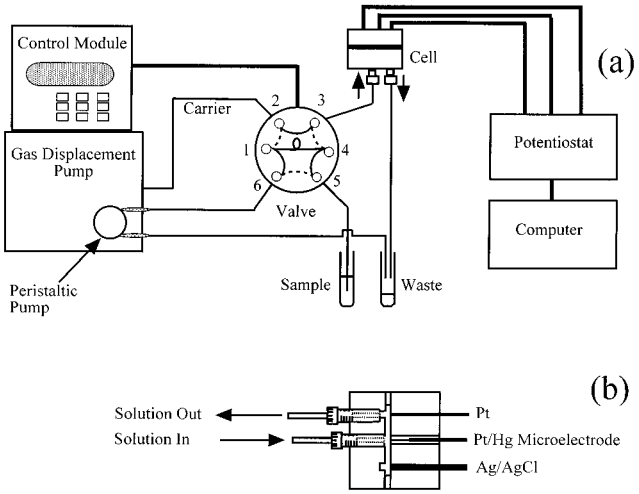

Figure 1. (a) Schematic representation of the microflow system for fast-scan anodic stripping voltammetry. The solid curves that connect the ports of the valve represent the configuration in which the valve is in load position, whereas the dotted curves show the configuration for injection. When the valve is in the inject position, the peristaltic pump will be turned on by the control module to fill the sample. The thick lines in the schematics are electrical cables, and the thin lines that interconnect the cell, the valve, and the gas displacement pump are Teflon-encapsulated PEEK tubings. (b) Schematic diagram of a cross section of the thin-layer flow-onto cell. The solution flowed onto the Hg microelectrode and exited through the groove from the outlet that was positioned directly across the Pt auxiliary electrode.

Electrodes and Cells. Pt microelectrodes were fabricated by sealing 10-μm-diameter Pt wires (Goodfellow Corp., Cambridge, England) into glass capillaries.[22] The electrodes were then tested and embedded with insulating epoxy (Epoxy Technologies, Billerica, MA) into PEEK blocks that also encapsulate the auxiliary and reference electrodes. The Pt microelectrode was polished with diamond paste down to 1 μm (Buehler, Lake Bluff, IL). The auxiliary electrode was a 1-mm-diameter Pt disk, and the reference electrode was a 1.5-mm-diameter Ag disk coated with a thin AgCl film. Formation of the thin AgCl film was accomplished by applying a small drop of coating solution (BAS, West Lafayette, IN) to the Ag electrode for 1 min. The potential at such a AgCl-coated Ag reference electrode was found to be stable and was 0.2 V more positive than a standard Ag/AgCl reference electrode in our carrier solution (containing no chloride). In this paper, all the voltammograms and potentials have been converted to the scale of the standard Ag/AgCl electrode.

The flow electrochemical cell has a flow-onto configuration (Figure 1b), similar to that in the BAS UniJet cell design (BAS, West Lafayette, IN)[23a] or the wall-jet flow cell developed as the electrochemical detector for HPLC.[23b] Two improvements were made: (1) a PEEK block (instead of a stainless steel one in the BAS UniJet cell design) with a groove of small volume (about 6 μL) was used, (2) the reference and auxiliary electrodes were positioned on each side of the working microelectrode (Figure 1b). These improvements were made because (i) PEEK is more suitable for trace metal analysis than stainless steel because of its low memory effects, and (ii) large volume (the groove in the UniJet has a volume of milliliter size) could increase the cell wash time at microbore flow rates, which in turn would lower the sample

(23) (a) Bohs, C. E.; Linhares, M. C.; Kissinger, P. T. *Curr. Sep.* **1994**, *13* (4), 6−8. (b) Fleet, B.; Little, C. J. *J. Chromatogr. Sci.* **1974**, *12*, 747−752.

throughput. Note that the consideration regarding the position of auxiliary electrode with respect to that of the microelectrode is no longer essential, since there should be little potential gradient across a microelectrode.

Procedure. Fresh solutions were prepared daily by weighing various amounts of standard solutions in polyethylene bottles and diluting with carrier solution. Carrier solution (0.02 M HNO_3) was deaerated and transferred into the GDP reservoir with a peristaltic pump. The general procedure for in situ deposition of Hg involved injecting into the flow cell from a 250-μL loop a 0.05 M KNO_3 solution containing 5 mM Hg^{2+} at 25 μL/min for 4 min while the potential at the Pt microelectrode was held at −0.2 V vs Ag/AgCl. The current−time curve for Hg deposition is very similar to that for Hg deposition in a quiescent solution reported by Wehmeyer and Wightman.[3] Such a similarity can be ascribed to the fact that the spherical diffusion is still the important, if not dominating, mass-transport mode in our system. The resulting Hg microelectrode was found to be hydrodynamically stable (for at least 7 h). We also found that small Hg droplets (Hg "sphere-caps", see below) of very similar radii (determined by the means described in Results and Discussion) can be made routinely by using the same deposition time at a fixed flow rate. After the Hg microelectrode formation, the 250-μL sample loop was replaced with a smaller sample loop (either 1.2 or 25 μL), and the degassed analyte solution was loaded. The electrode potential was then switched to the suitable deposition potential for the metal analytes, and FS-ASV was performed after the preconcentration step. A background voltammogram was collected immediately after each stripping analysis using the same experimental parameters.

RESULTS AND DISCUSSION

Parameters Affecting the Analytical Performance of Flow-Injection FS-ASV. (a) Dependencies of Solution Flow Rates. The low dependence of stripping peak currents (i_p) at microelectrodes on the solution flow rates, attributable to the convection-independent, steady-state diffusional contribution, has been reported in several studies.[17,24,25] In this study, it was proven that, at a flow rate of a few microliters per minute, the contribution of the fast diffusion process at microelectrodes constitutes more than half of the current. Figure 2a shows the voltammograms of 2.0 mM $Ru(NH_3)_6Cl_3$ at a Hg-coated Pt microelectrode at 25 μL/min (curve 3), at 4.9 μL/min (curve 2), and in a quiescent solution (curve 1). As can be seen, the steady-state current during the forward potential scans increased by only 1.4 times when the volume solution flow rate was changed from 4.9 to 25 μL/min (slightly more than a 5-fold increase). This low-volume solution flow rate dependency suggests that it would be more advantageous to conduct flow injection ASV at slower flow rates, since the sample consumption would be significantly reduced. This point is further elaborated in connection with the discussion about the flow injection FS-ASV experiments of Pb^{2+}. To estimate the net contribution to the total current by the rapid diffusion process at the Hg microelectrode, a pH 1.8 buffer solution containing 2.0 mM $Ru(NH_3)_6Cl_3$ was first injected into the cell, followed by stopping the solution flow (by turning the gas displacement pump off) and allowing sufficient time for the system to reach a stable quiescent condition. The voltammogram obtained under such a condition had a steady-state current of 34.5 nA, about 60% of the total current from the voltammogram obtained at 4.9 μL/min. The hysteresis between the forward and reverse potential scans in curve 1 is probably because depletion of the analyte becomes discernable at an electrode of relatively large geometric area. The area of the "Hg superhemisphere-cap" (see below) in Figure 2a is about 1.2 times of that of a 25-μm-diameter microdisk electrode (which is generally regarded as a larger microelectrode). Smaller hystereses in curves 2 and 3 (both were obtained under hydrodynamic conditions) support such a reasoning, because mass transport due to convection has minimized the effect of the analyte depletion in the vicinity of the electrode on the voltammetric response. It is worth mentioning that the current plateau (rather than current peaks) indicates that the spherical diffusion process at the Hg droplet is not hindered by the thin solution layer that is confined within the gap. This is because the thickness of the thin-layer gap in the cell (127 μm) is much greater than the size of the Hg microelectrode (the Hg "sphere-cap" microelectrodes had radii of, typically, a few micrometers); thin-layer electrochemical effects should not exist at the microelectrode on the short experimental time scale.[26] The high mass transport rate due to the spherical diffusion process is a unique feature, beneficial to the enhancement of the preconcentration efficiency, for ASV analysis.

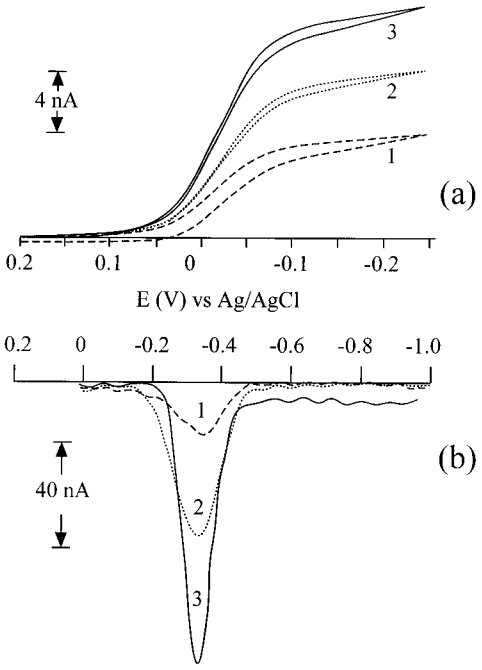

Figure 2. (a) Cyclic voltammograms of a 2.0 mM $Ru(NH_3)_6Cl_3$ in a pH 1.8 phosphate buffer at a Hg superhemisphere-cap microelectrode (a = 6.2 μm). The solid line curve (curve 3) was obtained when $Ru(NH_3)_6Cl_3$ was flowing onto the electrode at 25 μL/min, and the dotted line curve (curve 2) was acquired at 4.9 μL/min. The dashed voltammogram (curve 1) was obtained from a quiet solution containing $Ru(NH_3)_6Cl_3$ by injecting the sample at 4.9 μL/min, followed by stopping the flow of the carrier solution. The scan rate was 100 mV/s. (b) Fast-scan anodic stripping voltammograms acquired after preconcentrating Pb for 60 s from a 0.02 M HNO_3 solution containing 4.9×10^{-7} M Pb^{2+} at 25 μL/min (solid line curve, curve 3), at 4.9 μL/min (dotted line curve, curve 2), and after the solution flow was stopped (dashed line curve, curve 1). The scan rate was 5 V/s, and the deposition potential was −1.2 V vs Ag/AgCl.

(24) Caudill, W. L.; Howell, J. O.; Wightman, R. M. *Anal. Chem.* **1982**, *54*, 2532−2535.
(25) Bixler, J. W.; Bond, A. J. *Anal. Chem.* **1986**, *58*, 2859−2863.
(26) Kwak, J.; Bard, A. J. *Anal. Chem.* **1989**, *61*, 1221−1227.

Figure 2b further demonstrated that, indeed, it is desirable to use the slow volume flow rate for flow injection FS-ASV experiments. The i_p of the Pb stripping peak observed at 4.9 μL/min using a scan rate of 5 V/s (curve 2) decreased less than 50% with respect to that obtained at 25 μL/min (curve 3). The difference between the i_p of the analyte preconcentrated from a quiet solution (curve 1) and that preconcentrated in a flowing solution stream (e.g., curve 2) is more pronounced. Figure 2b shows that i_p of curve 1 is only one-third of the peak height of curve 2. The possibility of depletion of the analyte ions due to the long electrolysis in the thin solution layer was again ruled out, because the i_p remained essentially unchanged when larger thin-layer gaps were created. Creation of larger thin-layer gaps was accomplished, after curve 1 had been recorded, by disassembling the cell, adding another cell gasket, and then carefully remounting the cell blocks.

(b) Sizes of Hg "Sphere-Cap" Microelectrodes. It is generally believed that the cathodic deposition of Hg onto a disk microelectrode will result in the formation of a Hg film of a "sphere-cap" shape.[27] Since Hg wets a Pt disk microelectrode better than a carbon fiber electrode,[3,5] the basal plane of the sphere-cap is presumed to occupy the same area of the substrate disk electrode.[27] Alfred and Oldham have developed the theory[27] that can be used to deduce the radius of a Hg sphere-cap (a) from the ratio between the steady-state current at a Hg sphere-cap microelectrode and that can be calculated from a perfect hemispherical Hg microelectrode.[3] Hemispherical Hg microelectrode is a special Hg sphere-cap. Its radius a is equal to the radius of the substrate microelectrode (λ). The current arising from the hemispherical Hg microelectrode, i_H, is given by

$$i_H = 2\pi nFDC\lambda \qquad (1)$$

The new parameters in eq 1 are n, the number of electrons in the electrode reactions; F, Faraday's constant; D, the diffusion coefficient of the electroactive species; and C, the concentration of the electroactive species. Alfred and Oldham have tabulated the dimensionless radii, a/λ, as a function of the aforementioned steady-state current ratios.[27] A sphere-cap microelectrode whose a/λ is greater than 1 is referred to as a superhemisphere. If the a/λ ratio is less than 1, the sphere-cap is called a subhemisphere.

To estimate the radius of a sphere-cap electrode, we rely on the steady-state current of $Ru(NH_3)_6Cl_3$ obtained in a quiescent solution. For example, the voltammogram, depicted as curve 1 in Figure 2a, has a steady-state current during the forward potential scan corresponding to a 6.2-μm-radius superhemisphere-cap. Since hemispherical diffusion is still predominant at such a Hg superhemisphere-cap, it should be a good approximation to use the method to estimate the radius.

The radius of Hg sphere-cap was found to grow with the deposition time. When 5 mM Hg^{2+} was deposited onto a Pt microelectrode for 4 min at 25 μL/min, the radii of the resulting Hg sphere-caps were generally close to that of the two-thirds sphere.[27] Hg sphere-caps whose sizes are between that of the hemisphere ($a = 5$ μm for a 5-μm-radius Pt substrate) and that of the two-thirds sphere ($a = 5.8$ μm) appear to be the optimal size for achieving overall high preconcentration efficiency and peak resolution. FS-ASV performances at sphere-caps larger than the two-thirds sphere or smaller than the hemisphere were evaluated. High current background due to hydrogen evolution and small stripping peaks were normally observed at Hg subhemisphere-caps ($a < 5$ μm, produced by plating Hg for less than 2 min), suggesting that either the Pt disk had not been fully covered by Hg or the areas of the Hg droplets were too small. Deposition of Hg for longer than 6 min resulted in the formation of very large sphere-caps (usually $a > 8.5$ μm). Sphere-caps that are larger than the two-thirds sphere-cap have similar or slightly better preconcentration efficiency, as judged from the i_p values of analytes preconcentrated under the same experimental conditions. However, the stripping peaks were generally broader, and Cd and Pb peaks tend to merge at relatively fast scan rates (e.g., 10 V/s). Such a behavior is conceivable since the charging currents at larger electrodes become more significant at faster scan rates.

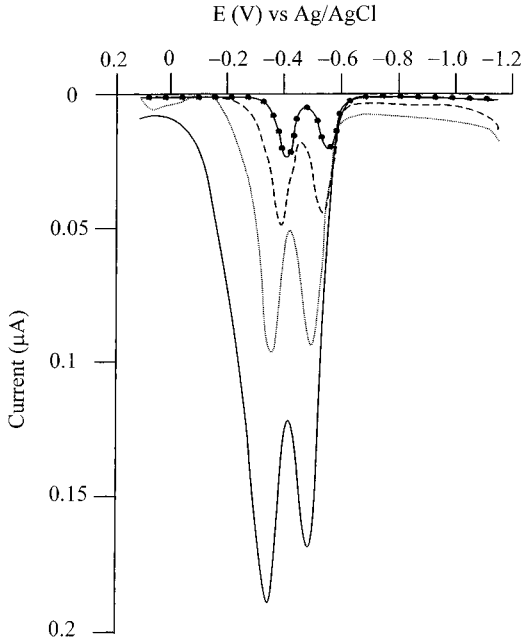

Figure 3. Fast-scan anodic stripping voltammograms of 8.9×10^{-7} M Cd^{2+} and 7.2×10^{-7} M Pb^{2+} obtained following a 60-s preconcentration at 4.9 μL/min using the following scan rates: 2 (curve with filled circles), 5 (dashed line curve), 10 (dotted line curve), and 25 V/s (solid line curve). The deposition potential was set at −1.4 V vs Ag/AgCl. The radius the Hg sphere-cap was 5.6 μm.

(c) Effect of Scan Rates. The effect of scan rates on the peak currents of the ASV voltammograms was studied. Shown in Figure 3 are a series of ASV voltammograms obtained at different scan rates ν (2, 5, 10, and 25 V/s), following a 60-s preconcentration of 8.9×10^{-7} M Cd^{2+} and 7.2×10^{-7} M Pb^{2+} at 4.9 μL/min. Two trends, which were reported in other studies related to FS-ASV at Hg microelectrodes[5] or thin Hg film electrodes,[28] can also be seen here: (1) i_p's of Cd and Pb increased almost linearly with ν within the range between 0.1 and 15 V/s. The slopes of the log i_p vs log ν plots are 0.80 for Pb and 0.81 for Cd, with correlation coefficients of 0.9970 and 0.9981, respectively. (2) Both the stripping peaks of Cd and Pb shifted in the anodic direction as the scan rate was increased. The shift for Cd is greater than that for Pb. For example, when ν was changed from 10 to 25 V/s, the Cd peak shifted about 16 mV, while the Pb peak shifted only 4 mV. The difference in the dependencies of the potential shifts of the cadmium and lead stripping peaks on scan

(27) Alfred, L. C. R.; Oldham, K. B. *J. Phys. Chem.* **1996**, *100*, 2170−2177.

(28) Wu, H. P. *Anal. Chem.* **1996**, *68*, 1639−1645.

rate may be attributable to the different kinetics of the chemical reactions occurring in amalgams. For example, it is generally believed that Cd interacts much more strongly with Pt at the Pt/Hg interface than Pb.[5] Because of the difference in the peak shifts and the higher charging currents at faster potential scan rates, the Cd and Pb stripping peaks merged almost completely at scan rates above 100 V/s (not shown). Very fast scan rates generally yield broader stripping peaks with smaller peak currents due to the higher charging current and less time for all the metals to strip within certain potential range (see the following discussion). The decrease in peak currents at faster scan rates can be used to explain the lower-than-one slopes of the log i_p vs log ν plots. Therefore, as far as the peak resolution and the linearity between i_p and ν are concerned, moderately fast scan rates (e.g., 5−15 V/s) are most suitable for achieving quantitative results.

Another factor that can possibly limit the use of very fast scan rates is "incomplete stripping". Incomplete stripping occurs only when the time scale of the fast potential scan is shorter than that for all the preconcentrated metals to diffuse out of the Hg sphere-cap.[29] The diffusion time (τ) of an analyte in Hg can be calculated by the following formula:

$$\tau = a^2/D \qquad (2)$$

D in eq 2 is the diffusion coefficient of the analyte in mercury (at 25 °C, D is 2.0×10^{-5} cm^2/s for Cd and 2.1×10^{-5} cm^2/s for Pb[20]). So, for the Hg superhemisphere-cap used to obtain Figure 3 ($a = 5.6\ \mu$m), the longest τ (analyte at the center of the sphere-cap) would be about 16 ms for Cd and 15 ms for Pb, whereas the time for the potential to scan over a typical stripping peak width at 25 V/s (approximately 0.3 V for Cd as determined from a separate solution containing only Cd) is 12 ms. Therefore, the data would probably be less quantitative at scan rates about 25 V/s or higher.

To verify the above assumption, we conducted two consecutive fast linear potential sweeps at 25 V/s, with the potentiostat preset at a high current sensitivity scale (e.g., 0.2 nA/V). The voltammogram recorded during the second potential scan yielded two distinct Cd and Pb stripping peaks, whose heights were about 6−10% of the i_p's of the voltammogram obtained in the first potential sweep. These peaks were absent in the voltammograms monitored at scan rates slower than 15 V/s. Therefore, we conclude that the Hg sphere-cap should be a good approximation for the shape of the Hg microelectrode, and very fast potential scans could yield less quantitative results due to incomplete stripping.

(d) Effect of Deposition Time. Similar to the relationship between i_p and scan rate, the peak current also increases linearly with the deposition time. Excellent linearity was found to hold for the concentration range we studied. For example, linear regression of the plot of i_p's obtained from preconcentrating 4.8×10^{-7} M Pb at 4.9 μL/min vs the deposition time yielded a slope of 110 nA/min and a correlation coefficient of 0.9993.

Analytical Aspects of Flow Injection FS-ASV. (a) Dynamic Range and Reproducibility. Flow injection FS-ASV of Pb^{2+} and Cd^{2+} at Pt-based Hg sphere-cap microelectrodes was found to possess wide dynamic ranges. The linearities in the ranges from 4.8×10^{-9} to 9.7×10^{-7} M for Pb^{2+} (or from 1 to 200 ppb) and from 4.4×10^{-9} to 1.8×10^{-6} M (or from 0.5 to 200 ppb) for Cd^{2+} were studied. We divided these ranges into the high-end (10−200 ppb) and the low-end (0.5−10 ppb) regions, since more deposition time would be needed for less concentrated analyte solutions. Slopes, with the correlation coefficients listed in the parentheses, for the high and low ends of the Pb concentration range are 0.328 (0.9979) and 0.707 nA/ppb (0.9832), respectively, while those for Cd are 0.555 (0.9998) and 0.854 nA/ppb (0.9974), respectively. Because the deposition time used for the low end of the concentration is longer than that for the high end, the slopes are larger (peak currents increase linearly with deposition time, as discussed in the preceding section). The good correlation coefficients of the plots indicate that the calibration curves are linear, and the flow injection FS-ASV experiments should be quantitative over a wide range of concentrations. The dynamic range of the flow injection FS-ASV is actually wider than the aforementioned. Good linearities can be extended to even lower concentrations. For example, a correlation coefficient of 0.9754 was determined over the Cd concentration range between 8.9×10^{-10} and 8.9×10^{-9} M. The slope of this linear plot was used to estimate the detection limit of Cd in the following section.

We also plotted the normalized i_p's vs concentrations normalized to the lowest analyte concentration. Good proportionality was obtained. For example, the plot for the high end of the Cd^{2+} concentration range has a slope of 1.10.

One of the advantages of using microelectrodes for ASV in quiet solutions is the high precision associated with the fast and uniform spherical diffusion process at the microelectrode surfaces.[3] Because of the slow and pulsation-free solution flow and the precise design of the flow-onto thin-layer cell, the mass-transfer process remains uniform in our flow injection FS-ASV system. As a result, the high precision observable in quiescent solutions was maintained. For example, the %RSD ($n = 5$) of the stripping peak currents measured from 0.5-min preconcentrations of a 8.9×10^{-7} M Cd^{2+} solution is 1.1%, whereas that obtained from 3-min preconcentrations of a 8.8×10^{-9} M Cd^{2+} sample is 2.0%. These %RSD values compare well with those obtained from other flow systems[16,17] or quiet solutions.[3,5]

(b) Detection Limits. The detection limits of Cd^{2+} and Pb^{2+} by flow injection FS-ASV are a relative analytical aspect since the peak currents increase with number of parameters, including scan rate, solution flow rate, and deposition time. We estimated the detection limits using experimental parameters that are practical and reasonable (i.e., low sample consumption and high throughput). With a 2-min preconcentration at 4.9 μL/min, the detection limit for Cd^{2+} was determined to be 1.7×10^{-10} M, or 0.19 pg for a 9.8-μL sample, based on the ratios between 3σ (σ, the standard deviation of the base line) and the slope of the Cd^{2+} calibration curve in the concentration range between 8.9×10^{-10} and 8.9×10^{-9} M. This detection limit is more than 2 orders of magnitude lower than that obtained by Matysik and Werner with the same length of preconcentration time.[17] Figure 4 shows the background-subtracted fast-scan stripping voltammogram of Cd preconcentrated from a 2.7×10^{-9} M solution. The background voltammogram, obtained by holding the electrode potential at the same value for Cd deposition while the carrier solution (blank) was injected for 2 min, is also presented. The excellent signal-to-noise ratio clearly shows that the flow injection FS-ASV is very sensitive. This detection limit also compares favorably to other studies conducted in quiescent solutions, particularly when the short preconcentration time (2 vs 10 min used in ref 3) and the low

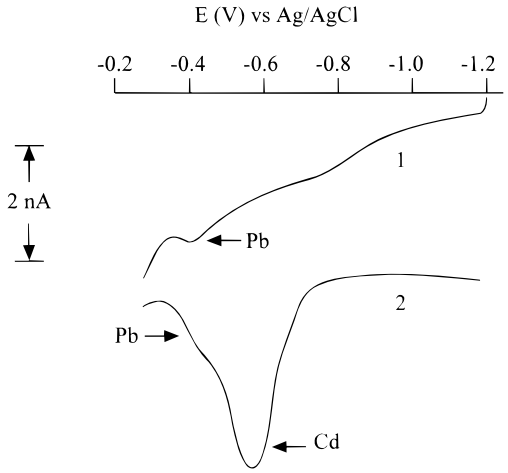

Figure 4. Background-subtracted, fast-scan anodic stripping voltammogram (curve 2) of 2.7×10^{-9} M Cd^{2+} that had been preconcentrated for 2 min at 4.9 μL/min. Deposition potential was −1.4 V vs Ag/AgCl, and the radius of the Hg superhemisphere was 6.0 μm. The background voltammogram (curve 1) was acquired after a 2-min deposition of a blank (carrier) solution.

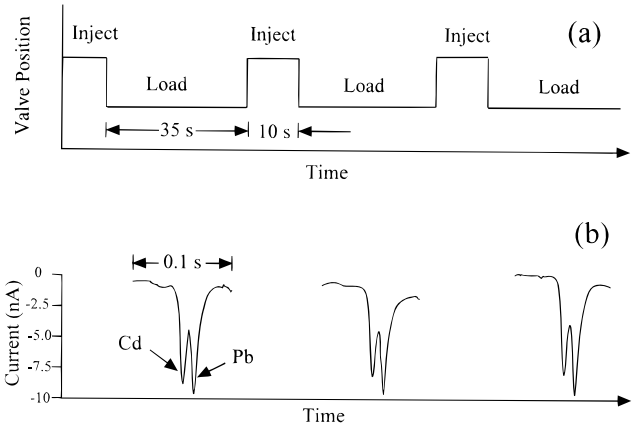

Figure 5. Schematic representation of fast-scan anodic stripping voltammetry conducted in a programmed procedure. Panel a shows a typical procedure consisting of three sequential loads and injections, and panel b depicts the corresponding background-subtracted fast-scan current−time curves. Experimental conditions: $[Cd^{2+}] = 8.9 \times 10^{-7}$ M and $[Pb^{2+}] = 7.2 \times 10^{-7}$ M; deposition potential was −1.4 V vs Ag/AgCl; and the radius of the Hg sphere-cap was 5.6 μm. The scan rate used was 10 V/s. The voltammograms were recorded 15 s after the valve was switched back to the load position.

sample consumption (less than 10 μL) are taken into consideration.

It was difficult for us to determine the Pb^{2+} detection limit because our carrier solution contained Pb^{2+} at the ultratrace level (probably subnanomolar or sub-parts-per-billion). The small shoulder of the Cd stripping peak (curve 2 in Figure 4) or the peak of the background voltammogram (curve 1) had a potential corresponding to that of the Pb stripping peak and was found to increase with the deposition time. For a 2-min preconcentration, i_p due to the trace lead in the carrier solution was at least 10 times less than that of the stripping peak obtained by preconcentrating a 4.8×10^{-9} M Pb^{2+} sample. Therefore, the Pb^{2+} detection limit of our flow injection FS-ASV system would be at subnanomolar levels or lower, if Pb^{2+} was absent in the carrier solution.

(c) Automation. Finally, potential utilization of this flow-injection FS-ASV system for automatic analysis was investigated. Figure 5 shows three background-subtracted fast-scan current−time curves obtained in a programmed procedure that has three sequential sample loadings and injections. An analyte solution containing 8.9×10^{-7} M Cd^{2+} and 7.2×10^{-7} M Pb^{2+} was first loaded into a 1.2-μL sample loop by the built-in peristaltic pump of the Microneb 2000. The valve was then switched to inject position for 10 s (the peristaltic pump was turned off by the control module at the same time), and the sample was delivered to the flow cell. Fifteen seconds after the injection, a potential scan at a rate of 10 V/s was initiated, and the preconcentrated metals were stripped into the carrier solution. After the stripping process, a background current−time curve was collected. Since Cd strips first, its stripping peak is on the left of the Pb peak when time is used as the basis to display the voltammogram. It was determined that 15 s was sufficient to ensure the whole injected sample plug passed the Hg microelectrode. With the valve in load position, the peristaltic pump was reactivated to fill the loop with the next sample.

In this experiment, each injection lasted for 10 s, with 0.82 μL of sample in the 1.2-μL loop consumed for one analysis. As can be seen in Figure 5b, the background-subtracted voltammograms are very reproducible. Each analysis takes only 45 s for submicromolar analyte concentrations. Although the microflow system and the potentiostat are controlled by separate computers, it should be straightforward to have the whole system integrated for fully automatic measuring routines.

CONCLUSION

This work has demonstrated that the combination of a low-dead-volume flow injection system with a miniaturized flow-onto thin-layer electrochemical cell dramatically reduces the sample consumption and significantly increases the sample throughput of anodic stripping analysis. For analyte concentrations that are in the submicromolar levels, only a few seconds is needed for the preconcentration step, consuming submicroliter samples. Also demonstrated here, for the first time, is that fast-scan voltammetry can be performed at a Hg sphere-cap microelectrode in a flowing solution stream for ultratrace metal analysis. Results obtained from the flow injection system/flow-onto thin-layer electrochemical cell, in conjunction with fast-scan voltammetry (flow injection FS-ASV), are reproducible and quantitative. The experimental setup for flow injection FS-ASV is fully computer-driven, and should be very suitable for routine automatic analysis.

ACKNOWLEDGMENT

F.Z. acknowledges the University of Wisconsin-Eau Claire (UWEC) for start-up funds and Research Corp. for students' support. We thank CETAC Technologies Inc. for providing the solution delivery and flow injection system (Microneb 2000) and CH Instruments for donating the electrochemical analyzer (CHI 832). Prof. David O. Wipf (Mississippi State University) is gratefully acknowledged for providing us the scanning electrochemical microscopy software (CE-6000) that can also be used to acquire fast-scan voltammograms.

Received for review July 30, 1996. Accepted December 11, 1996.[⊗]

AC960763Y

[⊗] Abstract published in *Advance ACS Abstracts,* February 1, 1997.